Phosphorylation and modulation of hyperpolarization-activated HCN4 channels by protein kinase A in the mouse sinoatrial node

Zhandi Liao,[1] Dean Lockhead,[1] Eric D. Larson,[1] and Catherine Proenza[1,2]

[1]Department of Physiology and Biophysics and [2]Department of Medicine, Division of Cardiology, University of Colorado, Anschutz Medical Campus, Aurora, CO 80045

The sympathetic nervous system increases heart rate by activating β adrenergic receptors and increasing cAMP levels in myocytes in the sinoatrial node. The molecular basis for this response is not well understood; however, the cardiac funny current (I_f) is thought to be among the end effectors for cAMP signaling in sinoatrial myocytes. I_f is produced by hyperpolarization-activated cyclic nucleotide–sensitive (HCN4) channels, which can be potentiated by direct binding of cAMP to a conserved cyclic nucleotide binding domain in the C terminus of the channels. β adrenergic regulation of I_f in the sinoatrial node is thought to occur via this direct binding mechanism, independent of phosphorylation. Here, we have investigated whether the cAMP-activated protein kinase (PKA) can also regulate sinoatrial HCN4 channels. We found that inhibition of PKA significantly reduced the ability of β adrenergic agonists to shift the voltage dependence of I_f in isolated sinoatrial myocytes from mice. PKA also shifted the voltage dependence of activation to more positive potentials for heterologously expressed HCN4 channels. In vitro phosphorylation assays and mass spectrometry revealed that PKA can directly phosphorylate at least 13 sites on HCN4, including at least three residues in the N terminus and at least 10 in the C terminus. Functional analysis of truncated and alanine-substituted HCN4 channels identified a PKA regulatory site in the distal C terminus of HCN4, which is required for PKA modulation of I_f. Collectively, these data show that native and expressed HCN4 channels can be regulated by PKA, and raise the possibility that this mechanism could contribute to sympathetic regulation of heart rate.

The Journal of General Physiology

INTRODUCTION

Each beat of the heart is initiated by spontaneous activity of myocytes in the sinoatrial node (SAN), and the sympathetic nervous system accelerates heart rate by increasing the spontaneous firing rate of sinoatrial myocytes. Both basal spontaneous pacemaker activity and the sympathetic "fight-or-flight" increase in heart rate are thought to depend on cAMP signaling within sinoatrial myocytes. However, the cAMP-sensitive pathways that control pacemaking are incompletely understood. Indeed, numerous proteins have been proposed as end effectors in this process (for review see Mangoni and Nargeot, 2008; see also Lakatta and DiFrancesco, 2009). Among the most prominent candidate proteins are hyperpolarization-activated cyclic nucleotide-sensitive (HCN) channels, which produce the cardiac funny current (I_f), and ryanodine receptors and other Ca^{2+} handling proteins, which are responsible for Ca^{2+} release from the sarcoplasmic reticulum. In this study, we focus on a novel mechanism for cAMP-dependent regulation of sinoatrial HCN channels.

There are four mammalian HCN isoforms (HCN1–4), with HCN4 being the main isoform in the sinoatrial node, where it is expressed at high levels (Shi et al., 1999; Moosmang et al., 2001; Marionneau et al., 2005; Liu et al., 2006). The related HCN1–3 isoforms are expressed primarily in neurons, where they produce hyperpolarization-activated currents known as I_h or I_q, which are thought to contribute to spontaneous activity, resting membrane potential, input resistance, and regulation of synaptic transmission (Biel, 2009; Moosmang et al., 1999). HCN channels are structurally similar to voltage-gated K^+ channels; they are tetramers, with each subunit composed of six transmembrane-spanning domains and large intracellular N and C termini. However, in contrast to K^+ channels, HCN channels conduct both Na^+ and K^+, and native HCN channels in mouse sinoatrial myocytes have a reversal potential of approximately −30 mV in physiological solutions (Mangoni and Nargeot, 2001; unpublished data). Thus, open HCN channels conduct a net inward current at diastolic potentials, and are consequently thought to contribute to spontaneous sinoatrial action potentials by depolarizing the membrane toward threshold during diastole.

Correspondence to Catherine Proenza: catherine.proenza@ucdenver.edu

Abbreviations used in this paper: CHO, Chinese hamster ovary; CNBD, cyclic nucleotide binding domain; HCN, hyperpolarization-activated cyclic-nucleotide sensitive; I_f, funny current; ISO, (−) isoproterenol (+) bitratrate; MS, mass spectrometry; PKI, protein kinase A inhibitory peptide 6-22 amide; SAN, sinoatrial node; WT, wildtype.

The Rockefeller University Press $30.00
J. Gen. Physiol. Vol. 136 No. 3 247–258
www.jgp.org/cgi/doi/10.1085/jgp.201010488

The large intracellular C terminus of HCN channels (~57% of the HCN4 sequence) contains a consensus cyclic nucleotide binding domain (CNBD). Binding of cAMP to the CNBD of HCN channels can shift the voltage dependence of activation to more positive potentials. In sinoatrial cells, sympathetic stimulation of β adrenergic receptors increases cAMP and shifts the voltage dependence of I_f to more positive potentials. It is generally thought that β adrenergic regulation of I_f is mediated by direct binding of cAMP to sinoatrial HCN channels, independent of phosphorylation (DiFrancesco and Tortora, 1991).

Whereas HCN channels can be regulated by direct binding of cAMP, ryanodine receptors and other Ca^{2+} handling proteins involved in sarcoplasmic reticulum Ca^{2+} release gain their cAMP sensitivity via phosphorylation by the cAMP-dependent protein kinase (PKA). These PKA-dependent Ca^{2+} release mechanisms have been proposed to be critical for basal and β adrenergic regulation of heart rate via a mechanism involving spontaneous Ca^{2+} release during diastole that triggers inward current through the Na^+–Ca^{2+} exchanger (Lakatta et al., 2010). The involvement of PKA or lack of involvement of direct cAMP binding to HCN channels has been used in attempts to discern the relative importance of Ca^{2+} release and I_f to sympathetic regulation of heart rate (Vinogradova et al., 2006; Harzheim et al., 2008). However, HCN channels contain numerous consensus PKA phosphorylation sites, and PKA has been shown to regulate the channels in some types of cells (Chang et al., 1991; Vargas and Lucero, 2002). These observations raise the possibility that PKA-dependent regulation of heart rate may include a contribution from HCN channels.

In this study, we tested the hypothesis that PKA can regulate sinoatrial HCN4 channels. We found that inhibition of PKA significantly impaired β adrenergic regulation of I_f in isolated murine sinoatrial myocytes, and that PKA potentiated heterologously expressed HCN4 channels. Using biochemistry and mass spectrometry (MS), we found that PKA can directly phosphorylate at least 13 sites in the N and C termini of HCN4. Functional studies of mutant channels demonstrated that a PKA regulatory site in the distal C terminus is required for PKA to shift the voltage dependence of HCN4. In addition, domains in both the N and C termini of the channels were found to contribute to the basal voltage dependence of HCN4 in the absence of PKA.

MATERIALS AND METHODS

Sinoatrial myocyte isolation

Sinoatrial myocytes were isolated from adult (>7 wk) male C57BL/6J mice in accordance with a protocol approved by the University of Colorado, Denver, Institutional Animal Care and Use Committee. Animals were injected with 225 µl intraperitoneal heparin (1000 U/ml). After 5 min, animals were anesthetized with isoflurane and euthanized by cervical dislocation. Hearts were quickly removed, the atria separated from the ventricles, and the sinoatrial node region dissected at 35°C in heparinized (10 U/ml) Tyrodes solution, which consisted of (in mM) 140 NaCl, 5.4 KCl, 1.2 KH_2PO_4, 5 HEPES, 5.55 glucose, 1 $MgCl_2$, 1.8 $CaCl_2$; pH adjusted to 7.4 with NaOH. The mouse sinoatrial node region was defined by the borders of the crista terminalis, the interatrial septum, and the superior and inferior vena cavae, as described in previous studies (Mangoni and Nargeot, 2001; Rose et al., 2004).

Nodal tissue was digested by collagenase type II (Worthington Biochemical), protease type XIV (Sigma-Aldrich), and elastase (Worthington Biochemical) for 25–30 min at 35°C in a modified Tyrodes solution (in mM: 140 NaCl, 5.4 KCl, 1.2 KH_2PO_4, 5 HEPES, 18.5 glucose, 0.066 $CaCl_2$, 50 taurine, 1 mg/ml BSA; pH adjusted to 6.9 with NaOH). After digestion, tissue was transferred to a modified KB solution (in mM: 100 potassium glutamate, 10 potassium aspartate, 25 KCl, 10 KH_2PO_4, 2 $MgSO_4$, 20 taurine, 5 creatine, 0.5 EGTA, 20 glucose, 5 HEPES, and 1.0% BSA; pH adjusted to 7.2 with KOH) at 35°C, and cells were dissociated by pipetting for 10 min with a wide fire-polished glass pipette. After gradual reintroduction of Ca^{2+}, dissociated cells were held at room temperature for up to 8 h before recording.

Sinoatrial myocyte electrophysiology

An aliquot of the sinoatrial cell suspension was transferred to a recording chamber on the stage of an inverted microscope, and individual sinoatrial myocytes were identified by spontaneous contractions, small size, and characteristic morphology (Fig. S1 A). Cells used in this study had action potentials typical of mouse sinoatrial cells (Fig. S1 B), and the membrane capacitance ranged from 22 to 52 pF, with the average being 34.7 ± 2.2 pF.

Hyperpolarization-activated I_f currents were recorded in the whole cell patch clamp configuration with pipettes that had resistances of ~1.5–3 MΩ when filled with an intracellular solution consisting of (in mM) 128 potassium aspartate, 6.6 sodium phosphocreatine, 7 KCl, 1 $MgCl_2$, 1 $CaCl_2$, 10 HEPES, 10 EGTA, 4 Mg-ATP; pH adjusted to 7.2 with KOH. All experiments were conducted at room temperature. PKA inhibitory peptide 6-22 amide (PKI; EMD) was stored as a frozen 10 mM stock solution (in water) and was added to the intracellular solution as noted to a final concentration of 10 µM. Once a gigaohm seal was established, cells were constantly perfused (~1–2 ml/min) with Tyrodes solution containing 1 mM Ba^{2+} to block K^+ currents. A 1 mM stock of (−) isoproterenol (+) bitratrate (ISO) was made fresh the day of each experiment, and was kept in the dark before being added to the Tyrodes solution to a final concentration of 1 µM, as indicated. We did not use $MnCl_2$ to block Ca^{2+} currents in our experiments, as it was observed to cause oxidation of the isoproterenol.

Conductance (g) for I_f was calculated as $g = I/(V_m - V_r)$, where I is the time-dependent component of inward current, V_m is the applied membrane voltage (corrected for a +14-mV junction potential error), and V_r is the reversal potential for I_f (−30 mV (Mangoni and Nargeot, 2001). Average conductance–voltage plots were fit with a Boltzmann equation to determine midpoint activation voltages ($V_{1/2}$):

$$f(V) = V_{min} + \frac{V_{max} - V_{min}}{1 + e^{\frac{Z_d F}{RT}(V - V_{1/2})}}$$

Molecular Biology

Four HCN4 GST fusion proteins were created by cloning in-frame into the pGEX-5x-1 plasmid (GE Healthcare) cDNA encoding amino acids 1–230, 528–737, 727–1008, and 917–1201 of HCN4 using EcoRI and XhoI restriction enzyme sites, which were

introduced by PCR. Four truncated HCN4 channels were created by inserting cDNA encoding amino acids 120–1201 (HCN4-ΔN), 1–718 (HCN4-ΔC), 120–718 (HCN4-ΔNΔC), and 1–1012 (HCN4-Δ1012) into the pcDNA3(+) plasmid (Invitrogen). A start codon was added to the 5′ end of HCN4-ΔN and HCN4-ΔNΔC clones. Serine to alanine point mutations in HCN4-Nx4 (S14A, S99A, S110A, and S117A) and HCN4-Cx4 (T1153A, S1154A, S1155A, and S1157A) were introduced by multiple rounds of overlapping PCR mutagenesis. DMSO (10%) was added to all PCR reactions to combat the high GC content (∼67% for the N- and C-terminal coding sequences) of the HCN4 cDNA, which is resistant to PCR. All clones were confirmed by automated DNA sequencing.

CHO cell culture, transfection, and electrophysiology

Chinese hamster ovary (CHO) cells were purchased from American Type Culture Collection and maintained in culture at 37°C and 5% CO_2 in a humidified incubator in Ham's F12 medium with 1% penicillin/streptomycin and 10% FBS (tetracycline screened). Cells from passages ∼3–12 were plated onto glass coverslips for electrophysiology. Transient transfection of cDNA encoding HCN channels (2 µg) along with the cell surface marker CD8 (1 µg) was performed using Fugene6 (Roche) according to the manufacturer's directions. Transiently transfected cells were identified by anti-CD8 antibody–coated beads (Invitrogen) (Jurman et al., 1994), and were used for electrophysiology 24–48 h post-transfection.

For some experiments, a stable CHO cell line expressing HCN4 under the control of a tetracycline-inducible promoter was used. In brief, cDNA encoding HCN4 was cloned into the pcDNA4/TO vector (Invitrogen), and TREX-CHO cells (which stably express the tetracycline repressor protein from the pcDNC4/TR plasmid; Invitrogen) were transfected as described above. Cells containing HCN4 and tetracycline repressor protein vectors were selected using Zeocin (250 µg/ml) and blasticidin (10 µg/ml), respectively. Expression of HCN4 channels was induced by addition of tetracycline (1–10 µg/ml) to the culture medium 24–48 h before recording.

For electrophysiological recordings, fragments of glass coverslips plated with HCN4-expressing CHO cells were transferred to a recording chamber (200 µl) on the stage of an inverted microscope. Cells were voltage clamped at room temperature in the whole-cell configuration using pipettes with resistances of ∼1.5–3 MΩ when filled with an intracellular solution that contained (in mM) 130 potassium aspartate, 10 NaCl, 1 EGTA, 5 HEPES, 0.5 $MgCl_2$, 2 MgATP; pH adjusted to 7.2 with KOH. Cells were constantly perfused (∼1–2 ml/min) with extracellular solution consisting of (in mM) 115 NaCl, 30 KCl, 1 $MgCl_2$, 1.8 $CaCl_2$, 5.5 glucose, 5 HEPES; pH adjusted to 7.4 with NaOH. Tail current amplitudes (elicited by steps to +60 mV) were plotted as a function of test potential (corrected for a +14-mV junction potential error), and the resulting conductance–voltage plots were fit with a Boltzmann equation as described above.

Native and expressed HCN channels are well known to experience rundown, which results in a negative shift in the voltage dependence of activation (e.g., DiFrancesco and Mangoni, 1994, Pian et al., 2006). To provide consistency in our measurements, we monitored rundown following break-in to whole cell mode using 1-s test pulses to −120 mV every 6 s both in HCN4-expressing CHO cells and in sinoatrial myocytes. Further experimental protocols (i.e., conductance–voltage protocols) were administered only after any decay of the current amplitude at −120 mV reached approximately steady state (usually 2–3 min).

GST fusion protein purification

pGEX plasmids with or without HCN4 inserts were transformed into competent BL21 cells (Agilent Technologies), and overnight cultures were grown at 37°C with shaking until the OD_{600} was between 0.5 and 0.7. Protein expression was induced with IPTG (0.1 mM) for 3–4 h at 37°C. Cells were then collected by centrifugation, resuspended in ice-cold PBS with protease inhibitors (Promega), and lysed by five freeze/thaw cycles. The resulting cell suspensions were incubated at 4°C in DNase I (10 µg/ml) and Triton X-100 (1%) with gentle rocking and were then centrifuged at 12,000 *g* for 30 min at 4°C. Supernatants were collected and incubated at 4°C with a 50% slurry of sepharose 4B beads (GE Healthcare). GST fusion proteins bound to the beads were dialyzed into PBS and stored at 4°C for up to 1 wk.

In vitro phosphorylation and mass spectrometry

Purified bead-bound GST fusion proteins were washed twice with a kinase assay buffer (in mM: 50 Tris, 10 NaF, 10 $MgCl_2$, 0.01 MgATP; pH adjusted to 7.5 with HCl) and were then incubated in "hot" kinase assay buffer, which contained 5 µCi of [γ-^{32}P]ATP (specific activity 25 mCi/mmol; MP Biomedicals) and 60 U of PKA catalytic subunit (EMD) for 1.5–2 h at 30°C. Reactions were stopped by boiling with 5X sample buffer at 95°C for 5 min. Proteins were then separated by SDS-PAGE and transferred to nitrocellulose membranes. Autoradiography was performed by overlaying the nitrocellulose with x-ray film for 0.5–26 h. Membranes were subsequently Western blotted with a rabbit anti-GST antibody (1:50,000; Oncogene), followed by an horseradish peroxidase–conjugated secondary antibody (1:10,000) for 1 h at room temperature. Bands were detected by chemiluminescence (Thermo Fisher Scientific).

Samples prepared for mass spectrometry were in vitro phosphorylated in kinase assay buffer (in mM: 50 Tris, 10 $MgCl_2$, 0.2 MgATP; pH adjusted to 7.5 with HCl) and separated by SDS-PAGE. Gels were stained with Coomassie brilliant blue, and bands of interest were excised and subjected to in-gel digestion with trypsin or trypsin plus chymotrysin followed by micro-capillary LC/MS/MS analysis (Taplin Mass Spectrometry Facility, Harvard Medical School).

Statistics

All results are reported as mean ± SEM. Comparisons were performed using two-tailed *t* tests.

Online supplemental material

Fig. S1 shows that cellular morphology and action potential shape for isolated murine sinoatrial myocytes are similar to those previously reported (Mangoni and Nargeot, 2001; Cho et al., 2003). Fig. S1 is available at http://www.jgp.org/cgi/content/full/jgp.201010488/DC1.

RESULTS

PKA contributes to β adrenergic regulation of I_f in sinoatrial myocytes

To determine whether PKA may contribute to β adrenergic regulation of I_f in sinoatrial myocytes, we recorded hyperpolarization-activated currents from isolated murine sinoatrial cells in the whole-cell patch-clamp configuration. Cellular morphology and action potential characteristics for our cells were similar to those previously reported for mouse sinoatrial myocytes (Fig. S1; Mangoni and Nargeot, 2001; Cho et al., 2003). As expected, the β adrenergic agonist ISO (1 µM) shifted the voltage dependence of I_f to more positive potentials. This shift was qualitatively apparent as an increase in I_f amplitude at −120 mV (near the activation midpoint for I_f) upon wash-on of ISO in the extracellular solution (Fig. 1, A and B). We next used the PKA pseudosubstrate

inhibitory peptide, PKI 6-22 amide (PKI, 10 μM) in the patch pipette to block PKA activity. Intracellular perfusion with PKI markedly reduced (in some cells; not depicted) or even eliminated the ability of ISO to potentiate I_f in sinoatrial myocytes (Fig. 1, C and D).

To quantitatively assess the effect of PKA on I_f, we determined the voltage dependence of activation for I_f with either ISO or ISO plus PKI. As shown in Fig. 2, ISO shifted the activation midpoint ($V_{1/2}$) of I_f to more depolarized potentials in myocytes perfused with the control intracellular solution (average shift = 11.3 ± 1.2 mV; $V_{1/2}$ = −129.3 ± 3.0 mV in Tyrode's, −118.1 ± 3.1 mV in ISO; n = 7; $P < 0.05$). Inclusion of PKI in the intracellular solution did not significantly alter the voltage dependence in the absence of ISO compared with the control intracellular. However, PKI significantly reduced the ability of ISO to modulate I_f (average shift = 3.7 ± 1.4 mV; $V_{1/2}$ = −125.3 ± 4.1 in Tyrode's with PKI, −121.6 ± 3.7 in ISO with PKI; n = 10; $P > 0.05$). While ISO had no statistically significant effect on $V_{1/2}$ in the presence of PKI, the data trended toward more positive values when ISO was applied, an observation that could be attributed to either incomplete block of PKA (perhaps due to limited perfusion of PKI in the SAN cells) or to direct binding of cAMP to the sinoatrial HCN channels.

As has been previously noted (e.g., Seifert et al., 1999), the very slow activation of I_f makes measurement of a true steady-state voltage dependence experimentally infeasible. Data presented in Fig. 2 were acquired using a voltage protocol consisting of 3-s steps to test potentials from −60 to −170 mV (Fig. 2 A, inset). The $V_{1/2}$ values generated in this way are useful in internal comparisons, but are difficult to compare with measurements made using other voltage protocols (e.g., in other studies). Moreover, the lack of steady-state current measurements means that changes in activation kinetics could masquerade as changes in voltage dependence. We thus examined time constants from double exponential fits of I_f at fully activated potentials for changes due to ISO or PKI. We found no significant effect of ISO or PKI on the rate of activation (not depicted), consistent with the classical notion that β adrenergic regulation of I_f occurs via a simple shift in the voltage dependence.

PKA shifts the voltage dependence of HCN4 in CHO cells

As a first step toward examining the mechanistic basis for PKA regulation of I_f, we next examined the functional effects of PKA on mouse HCN4 channels expressed in CHO cells. Hyperpolarization-activated currents were recorded in the whole-cell patch-clamp configuration in the presence or absence of the purified catalytic subunit of PKA (which lacks the cAMP-binding regulatory subunits and therefore is constitutively active, even in the absence of cAMP). As shown in Fig. 3, the voltage dependence of activation was significantly more positive when PKA (20 U/ml) was included in the intracellular solution ($V_{1/2}$ = −89.8 ± 1.7 mV, n = 7 in control intracellular, −83.8 ± 1.5 mV, n = 9 with PKA; $P < 0.05$). However, this difference was eliminated when PKI (10 μM) was included along with PKA in the patch pipette ($V_{1/2}$ in PKA + PKI = −90.0 ± 2.0 mV, n = 8; $P > 0.05$). These data are consistent with the above results showing PKA-dependent regulation of I_f in sinoatrial myocytes. Furthermore, the similarity in $V_{1/2}$ values in control versus PKA + PKI intracellular solutions suggests that background phosphorylation by any endogenous PKA in the CHO cells is minimal.

PKA phosphorylates multiple sites on HCN4

The above results indicate that PKA can regulate HCN4 channels, and that PKA activity is involved in

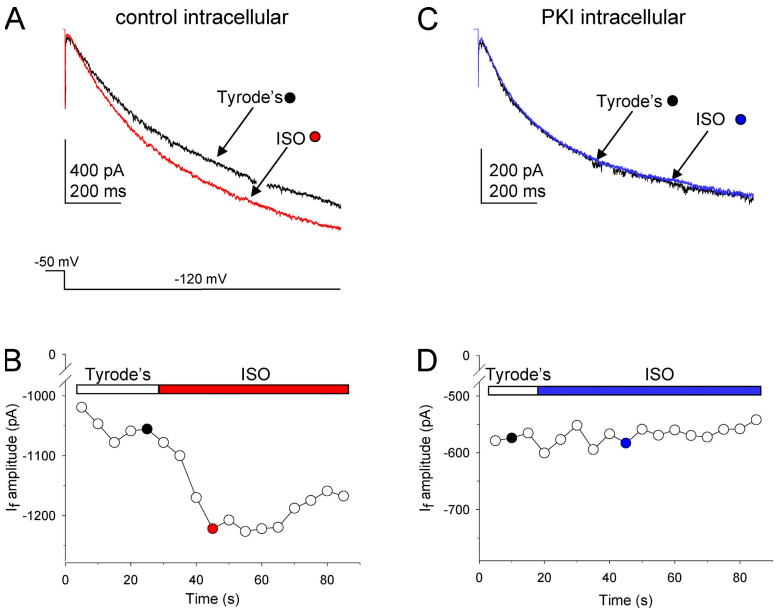

Figure 1. PKA activity contributes to β adrenergic regulation of I_f in sinoatrial myocytes. (A and C) Representative whole cell I_f currents recorded from isolated sinoatrial myocytes in the whole cell patch clamp configuration. Currents were elicited by voltage steps to −120 mV from a holding potential of −50 mV in the absence (black) or presence (red or blue) of 1 μM isoproterenol (ISO) applied in the extracellular Tyrode's solution. Traces in A were recorded with a control intracellular solution, traces in C were recorded with intracellular solution containing 10 μM PKI. (B and D) Time course of the ISO-dependent increase in I_f for the cells shown in A and C. The open and colored bars indicate the composition of the extracellular perfusing solution. Black, red, and blue circles mark the traces shown in A and C.

the communication between β adrenergic receptors and HCN4 channels in sinoatrial myocytes. However, they do not address whether PKA affects the channels directly or indirectly. Indeed, there are numerous PKA substrates within sinoatrial cells (and in CHO cells too) that could mediate this response. To determine whether PKA can directly phosphorylate HCN4, we next performed in vitro phosphorylation assays. Four GST fusion proteins were constructed, which consisted of portions of the intracellular N and C termini of HCN4: N-terminal residues 1–230 and C-terminal residues 528–737 (which includes the CNBD), 727–1008, and 917–1201 (Fig. 4 A; the C terminus was prepared as three overlapping fusion proteins because protein yields were very low for larger constructs). Purified GST fusion proteins were incubated with ^{32}P-ATP in the presence or absence of the catalytic subunit of PKA and in the presence or absence PKI (20 μM). As shown in the autoradiograph in Fig. 4 B (top), addition of PKA resulted in ^{32}P incorporation into each of the four of the HCN4 GST fusion proteins. ^{32}P was not incorporated into GST alone in any condition, or into any of the HCN4–GST fusion proteins in the absence of PKA. This indicated that the phosphorylation re-

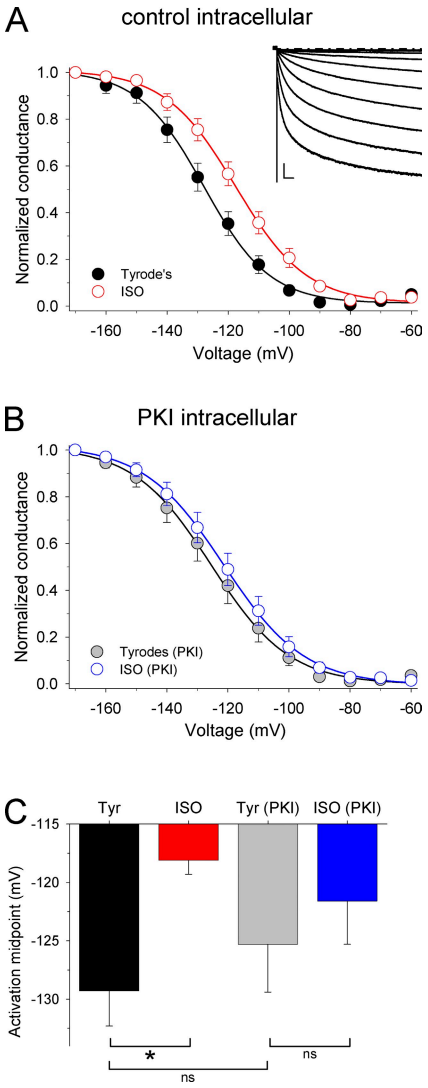

Figure 2. PKA inhibition reduces β adrenergic regulation of I_f in sinoatrial myocytes. (A and B) Conductance–voltage relationships for I_f determined in control intracellular solution (A) or intracellular containing 10 μM PKI (B) in the absence (closed black or gray symbols) and presence (open red or blue symbols) of 1 μM isoproterenol. (A, inset) Representative currents elicited by 3-s hyperpolarizing voltage steps from −60 to −170 mV in 10-mV increments. Scale bars in the inset are 500 pA and 200 ms. (C) Average activation midpoints for I_f in different conditions, as indicated. Isoproterenol significantly shifted the voltage dependence for I_f in the absence of PKI (asterisk, $P < 0.05$), but not in the presence of PKI (NS, not significant).

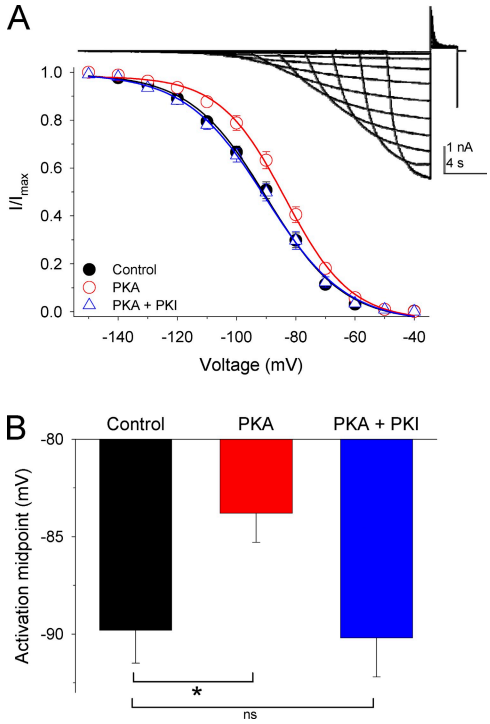

Figure 3. PKA shifts the voltage dependence of HCN4 in CHO cells. (A) Average voltage dependence of activation for HCN4 currents. Normalized tail current amplitudes are plotted as a function of prepulse voltage for protocols as shown in the inset with control intracellular solution (filled black circles), intracellular with 20 U/ml PKA (open red circles), or intracellular with PKA plus 10 μM PKI (open blue triangles). Midpoint activation voltages were −89.8 ± 1.7 mV in control, $n = 7$; −83.8 ± 1.5 mV in PKA, $n = 9$; and −90.0 ± 2.0 mV in PKA + PKI, $n = 8$. (Inset) Representative whole cell currents recorded from a CHO cell line stably expressing HCN4. Currents were elicited by hyperpolarizing voltage steps from −40 to −150 mV (in 10-mV increments), which ranged in length from 32.5 to 4.2 s (starting with the longest step at −40 mV and decremented by 2.575 s each step). This voltage protocol was used in an attempt to measure the steady-state voltage dependence of activation; however, note that activation was still incomplete at the more depolarized potentials. (B) Activation midpoints for HCN4 currents from Boltzmann fits to data in A. Asterisk indicates statistical significance ($P < 0.05$). NS, not significant ($P > 0.05$).

quired PKA and that it was associated with the channel moiety of the fusion proteins. Inhibition of PKA with PKI qualitatively reduced ^{32}P incorporation into each of the fusion proteins, to differing degrees.

Densitometric analysis was used to quantitate the PKA-dependent phosphorylation of HCN4. ^{32}P incorporation was evaluated as the pixel density of the autoradiograph bands for each construct (Fig. 4 B, top, dashed boxes), normalized to the density of the corresponding bands in the GST Western blots (Fig. 4 B, bottom) to correct for differences in gel loading. Mass spectrometry (see next section) confirmed that the selected bands corresponded to the full-length GST fusion proteins, despite the presence of degradation products. In Fig. 4 C, normalized phosphorylation averaged for three independent experiments is plotted for each construct. PKI significantly reduced the amount of ^{32}P taken up into the $C_{528–737}$ and $C_{727–1008}$ fusion proteins ($P < 0.05$). A trend toward reduction in ^{32}P activity was also seen in the presence of PKI for $N_{1–230}$ and $C_{917–1201}$. We believe that the lack of a significant decrease in band intensity by PKI for $N_{1–230}$ and $C_{917–1201}$ reflects incomplete inhibition of PKA for two reasons: (1) no phosphorylation of the GST fusion proteins was seen in the absence of PKA, and (2) mass spectrometry (see next section) revealed multiple phosphorylated residues in both $N_{1–230}$ and $C_{917–1201}$.

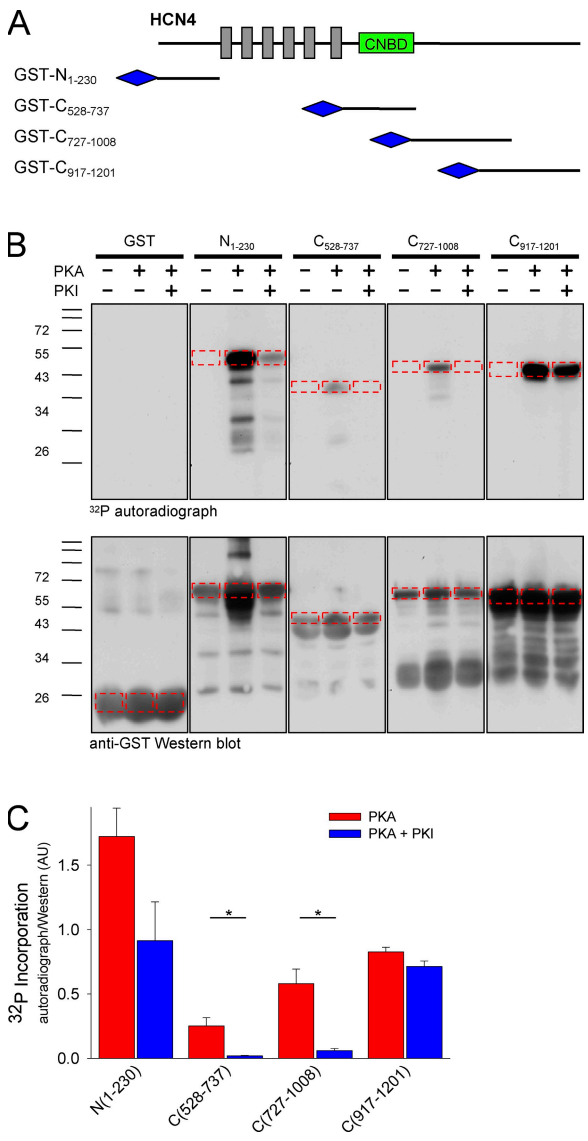

Figure 4. PKA phosphorylates HCN4 channel fragments in vitro. (A) Schematic representation of HCN4 GST fusion proteins. (B) In vitro phosphorylation and Western blotting of HCN4 channel fragments fused to GST. Fusion proteins were incubated with ^{32}P-ATP in the absence or presence of PKA (20 U/ml) or PKA plus PKI (20 µM) as indicated. Incorporated ^{32}P was visualized by autoradiography (top), and GST fusion proteins were visualized by Western blotting with an anti-GST antibody (1:50,000; Oncogene; bottom). (C) Average densitometric analysis of ^{32}P incorporation into the HCN4 GST fusion proteins for three independent experiments. Red bars show average density of ^{32}P normalized to the density of corresponding protein bands in the presence of PKA, blue bars, in PKA plus PKI. Asterisks indicate a significant reduction in normalized ^{32}P incorporation in the presence of PKI.

Identification of PKA sites by mass spectrometry

The in vitro phosphorylation data demonstrated that PKA can directly phosphorylate HCN4 at multiple sites. To identify the residues in the HCN4 N and C termini that can be phosphorylated by PKA, we used a mass spectrometry approach. We performed in vitro phosphorylation assays as above, except without the radioisotope. PKA-specific bands (i.e., those which were reduced in intensity by PKI in parallel lanes) from Coomassie-stained gels were excised, digested into peptides by trypsin or trypsin plus chymotrypsin, and subjected to liquid chromatography and tandem mass spectrometry (Taplin Biological Mass Spectrometry Facility, Harvard Medical School).

A total of 17 residues in HCN4 were found to be phosphorylated by PKA. Of these, 13 were considered "confirmed" by being present in at least two separate trypsin or trypsin/chymotrypsin fragments, and four were considered "unconfirmed," as they were identified in only single fragments. Fig. 5 shows the compiled peptide sequences for the HCN4 portions of the four GST fusion proteins compared with their target sequences. Red highlighted residues correspond to confirmed phosphorylation sites and green correspond to unconfirmed sites. The N terminus of HCN4 was phosphorylated at three confirmed sites (S14, S99, and S110), and at one unconfirmed site (S117). The C terminus of HCN4 was phosphorylated at a total of 13 sites, 10 confirmed (S719, S831, S918, S1005, S1051, T1071, S1128, T1153, S1154, and S1155) and 3 unconfirmed (S1011, S1112, and S1157).

Peptide sequencing (indicated by the bold underlined residues in Fig. 5) yielded the following coverage of the HCN4 portions of the GST fusion proteins (expressed as percentage of total amino acid count): $N_{1–230}$ = 95.2%, $C_{528–737}$ = 93.3%, $C_{727–1008}$ = 85.1%, and $C_{917–1201}$= 93.7%.

Gaps in the coverage include two serine or threonine residues in $N_{1–230}$, one in $C_{528–737}$, fourteen in $C_{727–1008}$, and three in $C_{917–1201}$. The large number of serine or threonine residues missing in $C_{727–1008}$ is mostly attributable to one gap in the sequence coverage, which persisted in three individual experiments, in both trypsin and trypsin/chymotrypsin digestions. While it is possible that one or more of the missed residues may be phosphorylated by PKA, it should be noted that none corresponds to predicted PKA sites (see below).

We compared the phosphorylated residues identified in HCN4 by mass spectrometry to high-scoring PKA sites predicted by the pkaPS algorithm, which evaluates target sequences in comparison to ∼20 flanking residues surrounding phosphorylation sites in known PKA substrate proteins (http://mendel.imp.ac.at/sat/pkaPS/; Neuberger et al., 2007). In Fig. 6, the 13 predicted PKA sites in HCN4 with scores ≥0.50 are indicated by yellow highlighting of residues in positions −6 to +1 relative to the candidate phosphate acceptor residue. The phosphorylated residues identified in our study are highlighted in red (confirmed) or green (unconfirmed), as in Fig. 5. 8 of the 13 confirmed phosphorylated residues identified by MS corresponded to highly scored pkaPS-predicted PKA phosphorylation sites (S14, S99, S719, S831, S1005, T1071, S1154, and S1155). This correspondence makes these positions particularly strong candidates for further analysis of PKA phosphorylation of HCN4 channels in vivo. On the other hand, four of the confirmed phosphorylated residues did not correspond to high-scoring PKA consensus sites, and five highly scored sites were not phosphorylated in our experiments. These differences could be due to the three dimensional structures of the GST fusion proteins, which do not conform to the native protein structure, or to false positives/negatives in the prediction algorithm. Of particular interest is residue S672 within the cyclic nucleotide binding domain, which had a pkaPS score of 1.20, yet was not phosphorylated in our assay. Mutations in this residue cause a hyperpolarizing shift in the voltage dependence of activation for I_f, and have been shown to be associated with familial sinus bradycardia (Milanesi et al., 2006).

PKA modulation of I_f requires a regulatory site in the distal C terminus

We next returned to functional assays to determine which (if any) of the residues identified by mass spectrometry mediate the PKA-dependent shift in voltage dependence of HCN4. Given the large number of sites, we began with a simple truncation strategy to first identify the region(s) of the HCN4 protein involved. Three truncated HCN4 channels were constructed: (1) HCN4-ΔN, in which approximately half of the N terminus was removed (residues 1–119) to eliminate the four potential PKA sites in the N terminus, (2) HCN4-ΔC, in which the C terminus was truncated just after residue 718 to eliminate all of the C-terminal PKA sites while leaving intact the CNBD, and (3) HCN4-ΔNΔC, which was a simple combination of the above deletions, and so lacked all the PKA-phosphorylated residues identified in the mass spectrometry analysis.

Deletion of all of the PKA sites in HCN4-ΔNΔC channels rendered the channels insensitive to PKA in functional assays (Fig. 7 B and Fig. 8). Hyperpolarization-activated

N_{1-203}

```
   1 MDKLPPSMRK RLYSLPQQVG AKAWIMDEEE DGEEEGAGGR QDPSRRSIRL RPLPSPSPSV
  61 AAGCSESRGA ALGATESEGP GRSAGKSSTN GDCRRFRGSL ASLGSRGGGS GGAGGGSSLG
 121 HLHDSAEERR LIAAEGDASP GEDRTPPGLA TEPERPATAA QPAASPPPQQ PPQPASASCE
 181 QPSADTAIKV EGGAAASDQI LPEAEVRLGQ SGFMQRQFGA MLQPGVNKFS
```

$C_{528-737}$

```
 528 QEKYKQVEQY MSFHKLPPDT RQRIHDYYEH RYQGKMFDEE SILGELSEPL REEIINFNCR
 588 KLVASMPLFA NADPNFVTSM LTKLRFEVFQ PGDYIIREGT IGKKMYFIQH GVVSVLTKGN
 648 KETKLADGSY FGEICLLTRG RRTASVRADT YCRLYSLSVD NFNEVLEEYP MMRRAFETVA
 708 LDRLDRIGKK NSILLHKVQH DLNSGVFNYQ
```

$C_{727-1008}$

```
 727 HDLNSGVFNY QENEIIQQIV RHDREMAHCA HRVQAAASAT PTPTPVIWTP LIQAPLQAAA
 787 ATTSVAIALT HHPRLPAAIF RPPPGPGLGN LGAGQTPRHP RRLQSLIPSA LGSASPASSP
 847 SQVDTPSSSS FHIQQLAGFS APPGLSPLLP SSSSSPPPGA CGSPPAPTPS TSTAAAASTT
 907 GFGHFHKALG GSLSSSDSPL LTPLQPGARS PQAAQPPPPL PGARGGLGLL EHFLPPPPSS
 967 RSPSSSPGQL GQPPGELSLG LAAGPSSTPE TPPRPERPSF MA
```

$C_{917-1201}$

```
 917 GSLSSSDSPL LTPLQPGARS PQAAQPPPPL PGARGGLGLL EHFLPPPPSS RSPSSSPGQL
 977 GQPPGELSLG LAAGPSSTPE TPPRPERPSF MAGASGGASP VAFTPRGGLS PPGHSPGPPR
1037 TFPSAPPRAS GSHGSLLLPP ASSPPPPQVP QRRGTPPLTP GRLTQDLKLI SASQPALPQD
1097 GAQTLRRASP HSSGESVAAF SLYPRAGGGS GSSGGLGPPG RPYGAIPGQH VTLPRKTSSG
1157 SLPPPLSLFG ARAASSGGPP LTTAAPQREP GARSEPVRSK LPSNL
```

Figure 5. Identification of PKA-phosphorylated residues in HCN4 GST fusion proteins. Compiled peptide sequences from tandem MS analysis of the HCN4 portions of the GST fusion proteins. Bold underlined residues were identified by MS sequencing; plain text residues were not resolved by MS. Red highlighting indicates residues found to be phosphorylated in multiple peptide fragments, and green highlighting indicates residues found to be phosphorylated in single peptide fragments.

currents produced by HCN4-ΔNΔC were qualitatively similar to currents produced by wild-type HCN4 (wtHCN4) channels, and the midpoint activation voltage for HCN4-ΔNΔC was not significantly different from that of wtHCN4 in the control intracellular solution (P = 0.669). However, PKA had no effect on the voltage dependence of HCN4-ΔNΔC ($V_{1/2}$ = −102.6 ± 1.7 mV, n = 8 in control, −100.0 ± 2.7 mV, n = 7 in PKA; P = 0.408). This is in contrast to wtHCN4, in which PKA significantly shifted $V_{1/2}$ to a more depolarized potential ($V_{1/2}$ = −101.3 ± 2.9, n = 5 in control, −89.1 ± 1.5 mV, n = 6 in PKA; P = 0.003; Fig. 7 A). (A shorter voltage protocol was used for these experiments compared with those shown in Fig. 3 [3-s hyperpolarizing steps vs. up to 30-s steps], which accounts for the difference in absolute $V_{1/2}$ values in Fig. 3 vs. Fig. 7. Note, however, that PKA significantly shifted the voltage dependence to more positive values, regardless of the voltage protocol.)

We next examined the role of the C terminus alone in the response of HCN4 to PKA. As for HCN4-ΔNΔC, PKA had no effect on the voltage dependence of HCN4-ΔC ($V_{1/2}$ = −122.9 ± 2.2 mV, n = 7 in control, −125.4 ± 1.6 mV, n = 6 in PKA; P = 0.399; Fig. 7 C and Fig. 8). Interestingly, however, $V_{1/2}$ in the absence of PKA was significantly more negative for HCN4-ΔC than for wtHCN4 or for HCN4-ΔNΔC (P ≤ 0.001). There was no significant difference in the kinetics of activation at fully activated potentials for HCN4-ΔC compared with wtHCN4 (unpublished data), suggesting that the observed difference in $V_{1/2}$ reflected primarily a difference in voltage dependence, not gating. Numerous explanations for this shift are possible, including nonspecific allosteric effects of the truncation, partial phosphorylation of wtHCN4 by endogenous PKA in CHO cells (although the lack of effect of PKI in Fig. 3 argues against the latter), or a potential functional interaction with the N terminus (see Discussion).

The above results suggested that the C terminus is required for PKA to shift the voltage dependence of HCN4. To test whether it is sufficient, we next examined functional effects of the N-terminal PKA sites identified by mass spectroscopy. Unfortunately, the HCN4-ΔN construct did not produce currents when transfected into CHO cells (a surprising result given the robust expression of HCN4-ΔNΔC). Western blot and immunocytochemistry suggested that very little HCN4-ΔN channel protein was expressed, and the protein that was expressed was not present at detectable levels on the plasma membrane (unpublished data). To circumvent the lack of expression of the truncated channel, we mutated the four putative N-terminal PKA sites to alanines (S14A, S99A, S110A, and S117A) to produce HCN4-Nx4 channels. PKA was found to significantly shift the voltage dependence of HCN4-Nx4 ($V_{1/2}$ = −112.7 ± 2.2 mV, n = 7 in control, −104.1 ± 2.6 mV, n = 8 in PKA; P = 0.03; Fig. 7 D), indicating that these residues are not necessary for PKA regulation of HCN4. The magnitude of the shift in Nx4 was not significantly (general linear interaction model, P = 0.4659) reduced compared with the shift in wtHCN4, making it unlikely that these residues contribute to PKA regulation of HCN4.

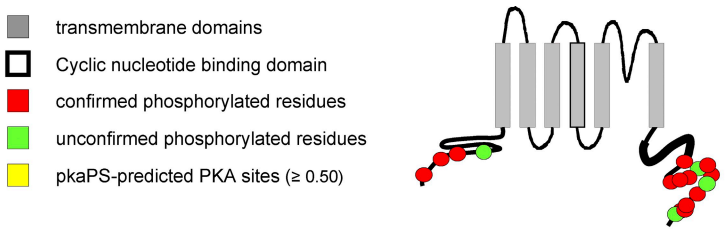


```
   1  MDKLPPSMRK RLYSLPQQVG AKAWIMDEEE DGEEEGAGGR QDPSRRSIRL RPLPSPSPSV
  61  AAGCSESRGA ALGATESEGP GRSAGKSSTN GDCRRFRGSL ASLGSRGGGS GGAGGGSSLG
 121  HLHDSAEERR LIAAEGDASP GEDRTPPGLA TEPERPATAA QPAASPPPQQ PPQPASASCE
 181  QPSADTAIKV EGGAAASDQI LPEAEVRLGQ SGFMQRQFGA MLQPGVNKFS LRMFGSQKAV
 241  EREQERVKSA GFWIIHPYSD FRFYWDLTML LLMVGNLIII PVGITFFKDE NTTPWIVFNV
 301  VSDTFFLIDL VLNFRTGIVV EDNTEIILDP QRIKMKYLKS WFVVDFISSI PVDYIFLIVE
 361  TRIDSEVYKT ARALRIVRFT KILSLLRLLR LSRLIRYIHQ WEEIFHMTYD LASAVVRIVN
 421  LIGMMLLLCH WDGCLQFLVP MLQDFPHDCW VSINGMVNNS WGKQYSYALF KAMSHMLCIG
 481  YGRQAPVGMS DVWLTMLSMI VGATCYAMFI GHATALIQSL DSSRRQYQEK YKQVEQYMSF
 541  HKLPPDTRQR IHDYYEHRYQ GKMFDEESIL GELSEPLREE IINFNCRKLV ASMPLFANAD
 601  PNFVTSMLTK LRFEVFQPGD YIIREGTIGK KMYFIQHGVV SVLTKGNKET KLADGSYFGE
 661  ICLLTRGRRT ASVRADTYCR LYSLSVDNFN EVLEEYPMMR RAFETVALDR LDRIGKKNSI
 721  LLHKVQHDLN SGVFNYQENE IIQQIVRHDR EMAHCAHRVQ AAASATPTPT PVIWTPLIQA
 781  PLQAAAATTS VAIALTHHPR LPAAIFRPPP GPGLGNLGAG QTPRHPRRLQ SLIPSALGSA
 841  SPASSPSQVD TPSSSSFHIQ QLAGFSAPPG LSPLLPSSSS SPPPGACGSP PAPTPSTSTA
 901  AAASTTGFGH FHKALGGSLS SSDSPLLTPL QPGARSPQAA QPPPPLPGAR GGLGLLEHFL
 961  PPPPSSRSPS SSPGQLGQPP GELSLGLAAG PSSTPETPPR PERPSEMAGA SGGASPVAFT
1021  PRGGLSPPGH SPGPPRTFPS APPRASQSHG SLLLPPASSP PPPQVPQRRG TPPLTPGRLT
1081  QDLKLISASQ PALPQDGAQT LRRASPHSSG ESVAAFSLYP RAGGGSGSSG GLGPPGRPYG
1141  AIPGQHVTLP RKTSSGSLPP PLSLFGARAA SSGGPPLTTA APQREPGARS EPVRSKLPSN
1201  L
```

Figure 6. Comparison of PKA-phosphorylated residues on HCN4 to predicted PKA phosphorylation sites. Amino acid sequence of mHCN4 is shown with color coding to illustrate phosphorylated residues identified by MS compared with predicted PKA sites. Red residues were phosphorylated in multiple peptide fragments, and green residues in single peptide fragments. Sequences identified as high probability PKA phosphorylation sites (score ≥ 0.5) by the pkaPS algorithm are highlighted in yellow. The cyclic nucleotide binding domain is indicated by a black outline, and transmembrane regions by gray shading. (Inset) Schematic representation of an HCN4 subunit with the approximate location of identified phosphorylated residues marked by red and green circles. The cyclic nucleotide binding domain is represented by a thick black line.

To further pinpoint the portion of the C terminus responsible for the PKA-dependent shift in $V_{1/2}$, we next constructed another deletion mutant in which the C terminus was truncated just after residue 1012, thereby eliminating six confirmed and two unconfirmed PKA sites while leaving four confirmed and one unconfirmed sites. We found that HCN4-Δ1012 channels were insensitive to PKA ($V_{1/2}$ = −109.2 ± 1.5, n = 7 in control, −109.8 ± 2.5 mV, n = 5 in PKA; Fig. 7 E), indicating that the PKA regulation requires only the distal C terminus of HCN4. Interestingly, $V_{1/2}$ for HCN4-Δ1012 was significantly more negative (P = 0.025) than for wtHCN4 and significantly more positive (P < 0.0001) than for HCN4-ΔC in the absence of PKA, suggesting the possibility that multiple domains within the C terminus could affect the voltage dependence of activation in the absence of PKA.

In the portion of the distal C terminus that was removed in HCN4-Δ1012, we were particularly intrigued by the cluster of four residues that were phosphorylated by PKA (T1153, S1154, S1155, and S1157), all of which lie within a single strong consensus PKA phosphorylation site. To test the importance of this PKA regulatory site in channel function, we mutated all four of these residues to alanines to produce HCN4-Cx4 channels. These four alanine substitutions eliminated the ability of PKA to shift the voltage dependence of HCN4-Cx4 channels ($V_{1/2}$ = −105.0 ± 3.7 mV, n = 8 in control, −107.5 ± 1.7 mV, n = 6 in PKA; Fig. 7 F and Fig. 8), indicating that this regulatory site is obligatory for modulation of HCN4 by PKA. The $V_{1/2}$ for HCN4-Cx4 in the absence of PKA did not differ from that of wtHCN4, suggesting that the C terminus must be intact for normal voltage gating of HCN4.

DISCUSSION

In this study, we found that PKA can regulate I_f in sinoatrial myocytes and in a heterologous expression system.

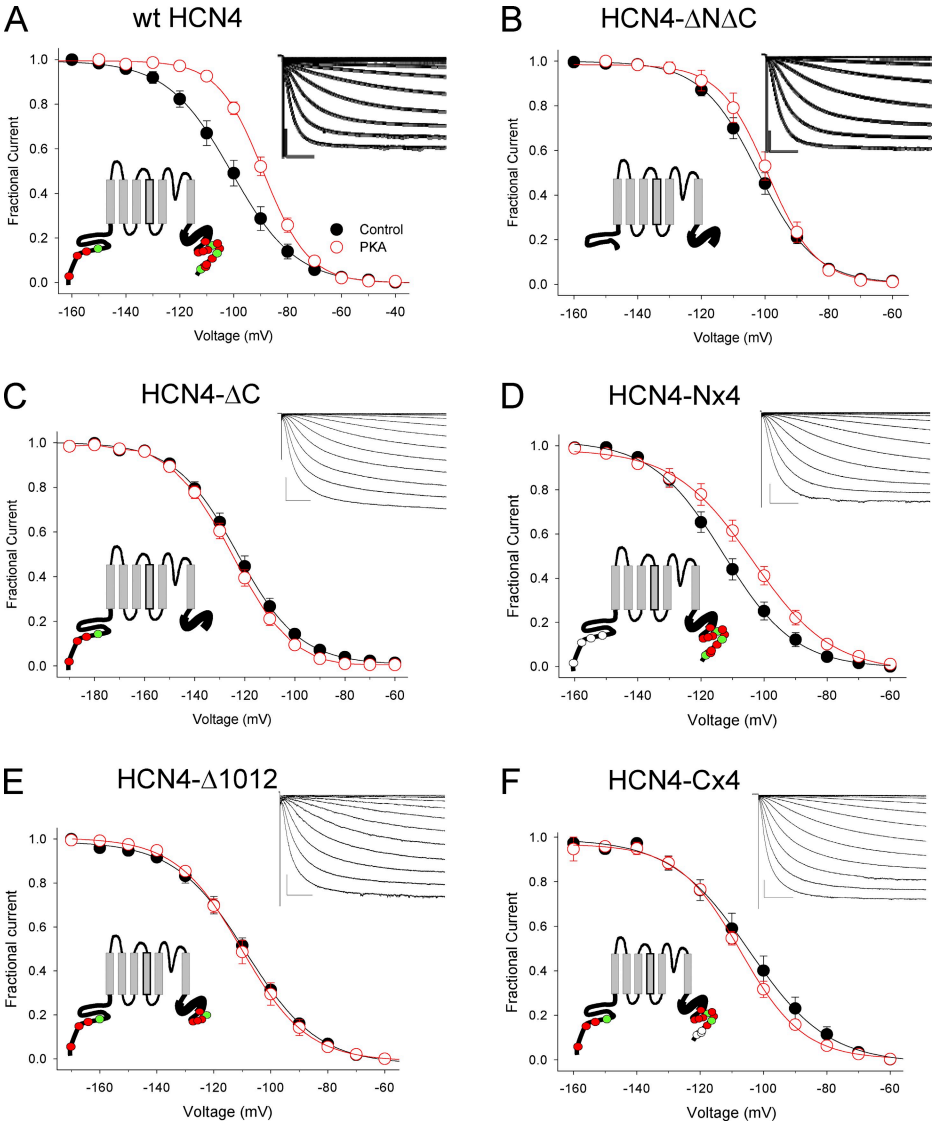

Figure 7. A regulatory site in the distal C terminus of HCN4 is required for PKA modulation. Representative whole-cell current traces (insets) and average conductance–voltage plots for wild-type HCN4 (A), HCN4-ΔNΔC (B), HCN4-ΔC (C), HCN4-Nx4 (D), HCN4-Δ1012 (E), and HCN4-Cx4 (F) expressed in CHO cells. Black lines and closed circles indicate control intracellular solution; red lines and open circles indicate PKA-containing intracellular solution. Currents were elicited by 3-s hyperpolarizing voltage steps ranging from −40 to −180 mV in 10-mV increments (as indicated). Scale bars: (A, B, and E, insets) 500 pA, 500 ms; (C, D, and F, insets) 1 nA, 500 ms. Cartoons in each panel depict the constructs, where red and green circles indicate confirmed and unconfirmed PKA sites, and open circles indicate alanine substitutions of PKA sites.

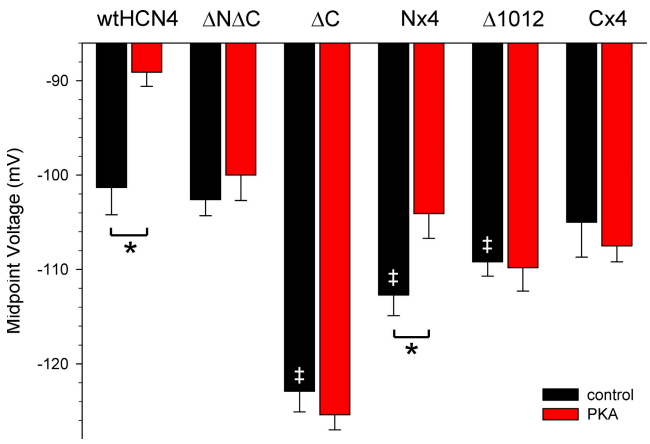

Figure 8. Summary of PKA-dependent shifts in $V_{1/2}$ for HCN4 constructs. Average activation midpoints from Bolztmann fits for wtHCN4, HCN4-ΔNΔC, and HCN4-ΔC in the absence (black bars) or presence (red bars) of 20 U/ml PKA in the intracellular pipette solution. Asterisks indicate statistical significance ($P < 0.05$) between control and PKA intracellular solution. Double daggers indicate significant differences from wtHCN4 in the absence of PKA.

We identified at least 13 residues in the intracellular N and C termini of HCN4 that can be phosphorylated by PKA in vitro. Functional analysis of mutant channels showed that a PKA regulatory site in the distal C terminus of HCN4 is required for PKA modulation of I_f. Overall, these data suggest that β adrenergic regulation of I_f in the sinoatrial node may occur via multiple cAMP-dependent mechanisms. The presence of consensus PKA sites in the other mammalian HCN isoforms hints that neuronal I_h currents may be similarly regulated by PKA signaling.

Phosphorylation-dependent versus phosphorylation-independent regulation of I_f

How can we reconcile our data with the prevailing notion that β adrenergic regulation of I_f is phosphorylation independent? This idea is based on the following observations: (1) cAMP can shift the voltage dependence of I_f even in the presence of kinase inhibitors or the absence of PKA cofactors (DiFrancesco and Tortora, 1991); (2) the cAMP analogue Rp-cAMP, which does not activate PKA, can shift the voltage dependence of I_f (albeit to a lesser degree than cAMP itself) (Bois et al., 1997); and (3) point mutations in the CNBD can render heterologously expressed HCN channels or I_f in embryonic mouse cardiomyocytes insensitive to cAMP (Chen et al., 2001; Harzheim et al., 2008). While these previous studies support the idea that direct binding of cAMP can regulate HCN4, explanations consistent with additional phosphorylation-dependent regulation of I_f are possible in each case. For example, direct effects of cAMP and Rp-cAMP on I_f were studied in excised inside-out patches from rabbit SAN cells, whereas our study used whole-cell recording from mouse SAN cells. Thus, one possibility is that there is a species-dependent difference in I_f regulation in mice versus rabbits. Differences in experimental preparations could also explain differing results. For instance, cAMP signaling is likely to differ in embryonic cardiomyocytes compared with adult sinoatrial myocytes, and PKA may simply be absent from excised membrane patches or tissue culture cell lines.

There is precedent for the idea that PKA may regulate HCN channels in some systems. For instance, kinase blockers were shown to abolish β adrenergic and cAMP-dependent regulation of I_f in canine Purkinje cells in two-electrode voltage-clamp experiments (Chang et al., 1991), and to shift the voltage dependence of I_h in rat olfactory neurons in whole-cell voltage-clamp experiments (Vargas and Lucero, 2002). On the other hand, the purified catalytic subunit of PKA had no effect on I_h in whole-cell voltage-clamp experiments in rat dorsal root ganglion cells (Komagiri and Kitamura, 2007) and guinea pig sensory afferent neurons (Ingram and Williams, 1996). Thus, it seems that regulation of cardiac and neuronal HCN channels by PKA may depend on the cellular context and/or the HCN channel isoform expression. It is noteworthy that all the mammalian HCN isoforms contain strong consensus PKA phosphorylation sites (the pkaPS algorithm predicts 15 sites with scores ≥0 in each HCN1 and HCN3, and 18 such sites in HCN2). This suggests that PKA may also regulate neuronal HCN channels, although differences in the distribution of the predicted sites hint that PKA could have distinct effects on each isoform.

Several studies have concluded that I_f may be irrelevant for autonomic control of heart rate based on data showing no effect on β adrenergic regulation of heart rate in heterozygous $HCN4^{+/R669Q}$ mice bearing a mutation in the CNBD (Harzheim et al., 2008), and showing that PKA activity appears to be obligatory for pacemaking (Vinogradova et al., 2006). However, these interpretations are based on the assumption that the only mechanism by which β receptors can modulate I_f is via direct binding of cAMP to sinoatrial HCN channels. Our present data neither support nor refute a role for I_f in β adrenergic regulation of pacemaking (which undoubtedly involves many redundant and interrelated mechanisms). However, by demonstrating that PKA can regulate I_f, our results allow the possibility that this signaling pathway may be among those involved in β adrenergic regulation of heart rate.

Biophysical implications for HCN4 channel function

Two unexpected observations in our study suggest that there may be a functional interaction between the N and C termini of HCN4 that can affect the expression and biophysical properties of the channel. First, the N-terminal deletion mutant, HCN4-ΔN, did not produce current, whereas, paradoxically, current density was

similar to wtHCN4 for the double truncation mutant, HCN4-ΔNΔC (in which both N and C termini were deleted). Second, the voltage dependence of HCN4-ΔNΔC did not differ from wtHCN4 in the absence of PKA even though the voltage dependence was hyperpolarized in both the C-terminal deletion mutant, HCN4-ΔC, and the N-terminal four-alanine substitution mutant, HCN4-Nx4. Physical and/or functional interactions have been reported for the N and C termini of several other ion channels, including cyclic nucleotide gated channels (Varnum and Zagotta, 1997; Zheng et al., 2003), small conductance Ca^{2+}-activated K^+ channels (Frei et al., 2006), bestrophin 1 Cl^- channels (Qu et al., 2009), and Kv2.1 K^+ channels (Mohapatra et al., 2008). Interestingly, the interaction between the N and C termini of Kv2.1 appears to be necessary for their modulation by phosphorylation. It will be interesting in future work to explore the mechanistic bases for the differences between HCN4-ΔNΔC and mutants lacking only the N or C termini.

The lack of expression of HCN4-ΔN was also somewhat surprising in light of our previous studies showing that only the proximal N terminus was necessary for functional expression of HCN2 (Proenza et al., 2002; Tran et al., 2002); HCN2 channels expressed at normal levels, provided the ∼50 residues adjacent to the first transmembrane segment were present. This region of the N terminus is conserved in all four mammalian HCN isoforms and was intact in the HCN4-ΔN construct used in the present study, suggesting that there are additional regions, unique to HCN4, that also control expression. The N terminus of HCN4 is considerably longer than that of the other HCN isoforms, and contains a proline-rich region (a hallmark of many protein interaction motifs) in addition to the four potential PKA phosphorylation sites we identified by mass spectrometry. Thus, it is possible that expression of HCN4 is regulated by phosphorylation and/or protein–protein interactions of the N terminus.

In this study, PKA regulation of I_f voltage dependence was shown to depend on four residues within a PKA regulatory site in the distal C terminus of HCN4. Determination of how each of these residues contributes to regulation of voltage dependence awaits characterization of single and multiple point mutants. More importantly, it remains to be determined as to which (if any) of these sites are relevant for physiological regulation of I_f in sinoatrial myocytes.

We gratefully thank Robert Rose for sharing his protocol for the isolation of mouse sinoatrial myocytes, Randall Walikonis for assistance with the in vitro phosphorylation experiments, Payam Andalib for initial studies, Roger Bannister for comments on the manuscript, and the University of Colorado Neuroscience Program core facilities for machine shop support.

This work was supported in part by grants to Catherine Proenza from the National Institutes of Health (HL088427) and the American Heart Association (0735614T).

Angus C. Nairn served as editor.

Submitted: 16 June 2010
Accepted: 02 July 2010

REFERENCES

Biel, M. 2009. Cyclic nucleotide-regulated cation channels. *J. Biol. Chem.* 284:9017–9021. doi:10.1074/jbc.R800075200

Bois, P., B. Renaudon, M. Baruscotti, J. Lenfant, and D. DiFrancesco. 1997. Activation of f-channels by cAMP analogues in macropatches from rabbit sino-atrial node myocytes. *J. Physiol.* 501:565–571. doi:10.1111/j.1469-7793.1997.565bm.x

Chang, F., I.S. Cohen, D. DiFrancesco, M.R. Rosen, and C. Tromba. 1991. Effects of protein kinase inhibitors on canine Purkinje fibre pacemaker depolarization and the pacemaker current i(f). *J. Physiol.* 440:367–384.

Chen, S., J. Wang, and S.A. Siegelbaum. 2001. Properties of hyperpolarization-activated pacemaker current defined by coassembly of HCN1 and HCN2 subunits and basal modulation by cyclic nucleotide. *J. Gen. Physiol.* 117:491–504. doi:10.1085/jgp.117.5.491

Cho, H.S., M. Takano, and A. Noma. 2003. The electrophysiological properties of spontaneously beating pacemaker cells isolated from mouse sinoatrial node. *J. Physiol.* 550:169–180. doi:10.1113/jphysiol.2003.040501

DiFrancesco, D., and M. Mangoni. 1994. Modulation of single hyperpolarization-activated channels (i(f)) by cAMP in the rabbit sino-atrial node. *J. Physiol.* 474:473–482.

DiFrancesco, D., and P. Tortora. 1991. Direct activation of cardiac pacemaker channels by intracellular cyclic AMP. *Nature.* 351:145–147. doi:10.1038/351145a0

Frei, E., I. Spindler, S. Grissmer, and H. Jager. 2006. Interactions of N-terminal and C-terminal parts of the small conductance Ca2+ activated K+ channel, hSK3. *Cell. Physiol. Biochem.* 18:165–176. doi:10.1159/000097665

Harzheim, D., K.H. Pfeiffer, L. Fabritz, E. Kremmer, T. Buch, A. Waisman, P. Kirchhof, U.B. Kaupp, and R. Seifert. 2008. Cardiac pacemaker function of HCN4 channels in mice is confined to embryonic development and requires cyclic AMP. *EMBO J.* 27:692–703. doi:10.1038/emboj.2008.3

Ingram, S.L., and J.T. Williams. 1996. Modulation of the hyperpolarization-activated current (Ih) by cyclic nucleotides in guinea-pig primary afferent neurons. *J. Physiol.* 492:97–106.

Jurman, M.E., L.M. Boland, Y. Liu, and G. Yellen. 1994. Visual identification of individual transfected cells for electrophysiology using antibody-coated beads. *Biotechniques.* 17:876–881.

Komagiri, Y., and N. Kitamura. 2007. Comparison of effects of PKA catalytic subunit on I(h) and calcium channel currents in rat dorsal root ganglion cells. *Biomed. Res.* 28:177–189. doi:10.2220/biomedres.28.177

Lakatta, E.G., and D. DiFrancesco. 2009. What keeps us ticking: a funny current, a calcium clock, or both? *J. Mol. Cell. Cardiol.* 47:157–170. doi:10.1016/j.yjmcc.2009.03.022

Lakatta, E.G., V.A. Maltsev, and T.M. Vinogradova. 2010. A coupled SYSTEM of intracellular Ca2+ clocks and surface membrane voltage clocks controls the timekeeping mechanism of the heart's pacemaker. *Circ. Res.* 106:659–673. doi:10.1161/CIRCRESAHA.109.206078

Liu, J., H. Dobrzynski, J. Yanni, M.R. Boyett, and M. Lei. 2006. Organisation of the mouse sinoatrial node: structure and expression of HCN channels. *Cardiovasc. Res.* 73:729–738.

Mangoni, M.E., and J. Nargeot. 2001. Properties of the hyperpolarization-activated current (I(f)) in isolated mouse sino-atrial cells. *Cardiovasc. Res.* 52:51–64. doi:10.1016/S0008-6363(01)00370-4

Mangoni, M.E., and J. Nargeot. 2008. Genesis and regulation of the heart automaticity. *Physiol. Rev.* 88:919–982. doi:10.1152/physrev.00018.2007

Marionneau, C., B. Couette, J. Liu, H. Li, M.E. Mangoni, J. Nargeot, M. Lei, D. Escande, and S. Demolombe. 2005. Specific pattern of ionic channel gene expression associated with pacemaker activity in the mouse heart. *J. Physiol.* 562:223–234. doi:10.1113/jphysiol.2004.074047

Milanesi, R., M. Baruscotti, T. Gnecchi-Ruscone, and D. DiFrancesco. 2006. Familial sinus bradycardia associated with a mutation in the cardiac pacemaker channel. *N. Engl. J. Med.* 354:151–157. doi:10.1056/NEJMoa052475

Mohapatra, D.P., D.F. Siino, and J.S. Trimmer. 2008. Interdomain cytoplasmic interactions govern the intracellular trafficking, gating, and modulation of the Kv2.1 channel. *J. Neurosci.* 28:4982–4994. doi:10.1523/JNEUROSCI.0186-08.2008

Moosmang, S., M. Biel, F. Hofmann, and A. Ludwig. 1999. Differential distribution of four hyperpolarization-activated cation channels in mouse brain. *Biol. Chem.* 380:975–980. doi:10.1515/BC.1999.121

Moosmang, S., J. Stieber, X. Zong, M. Biel, F. Hofmann, and A. Ludwig. 2001. Cellular expression and functional characterization of four hyperpolarization-activated pacemaker channels in cardiac and neuronal tissues. *Eur. J. Biochem.* 268:1646–1652. doi:10.1046/j.1432-1327.2001.02036.x

Neuberger, G., G. Schneider, and F. Eisenhaber. 2007. pkaPS: prediction of protein kinase A phosphorylation sites with the simplified kinase-substrate binding model. *Biol. Direct.* 2:1. doi:10.1186/1745-6150-2-1

Pian, P., A. Bucchi, R.B. Robinson, and S.A. Siegelbaum. 2006. Regulation of gating and rundown of HCN hyperpolarization-activated channels by exogenous and endogenous PIP2. *J. Gen. Physiol.* 128:593–604. doi:10.1085/jgp.200609648

Proenza, C., N. Tran, D. Angoli, K. Zahynacz, P. Balcar, and E.A. Accili. 2002. Different roles for the cyclic nucleotide binding domain and amino terminus in assembly and expression of hyperpolarization-activated, cyclic nucleotide-gated channels. *J. Biol. Chem.* 277:29634–29642. doi:10.1074/jbc.M200504200

Qu, Z., W. Cheng, Y. Cui, Y. Cui, and J. Zheng. 2009. Human disease-causing mutations disrupt an N-C-terminal interaction and channel function of bestrophin 1. *J. Biol. Chem.* 284:16473–16481. doi:10.1074/jbc.M109.002246

Rose, R.A., A.E. Lomax, C.S. Kondo, M.B. Anand-Srivastava, and W.R. Giles. 2004. Effects of C-type natriuretic peptide on ionic currents in mouse sinoatrial node: a role for the NPR-C receptor. *Am. J. Physiol. Heart Circ. Physiol.* 286:H1970–H1977. doi:10.1152/ajpheart.00893.2003

Seifert, R., A. Scholten, R. Gauss, A. Mincheva, P. Lichter, and U.B. Kaupp. 1999. Molecular characterization of a slowly gating human hyperpolarization-activated channel predominantly expressed in thalamus, heart, and testis. *Proc. Natl. Acad. Sci. USA.* 96:9391–9396. doi:10.1073/pnas.96.16.9391

Shi, W., R. Wymore, H. Yu, J. Wu, R.T. Wymore, Z. Pan, R.B. Robinson, J.E. Dixon, D. McKinnon, and I.S. Cohen. 1999. Distribution and prevalence of hyperpolarization-activated cation channel (HCN) mRNA expression in cardiac tissues. *Circ. Res.* 85:e1–e6.

Tran, N., C. Proenza, V. Macri, F. Petigara, E. Sloan, S. Samler, and E.A. Accili. 2002. A conserved domain in the NH2 terminus important for assembly and functional expression of pacemaker channels. *J. Biol. Chem.* 277:43588–43592. doi:10.1074/jbc.M208477200

Vargas, G., and M.T. Lucero. 2002. Modulation by PKA of the hyperpolarization-activated current (Ih) in cultured rat olfactory receptor neurons. *J. Membr. Biol.* 188:115–125. doi:10.1007/s00232-001-0178-y

Varnum, M.D., and W.N. Zagotta. 1997. Interdomain interactions underlying activation of cyclic nucleotide-gated channels. *Science.* 278:110–113. doi:10.1126/science.278.5335.110

Vinogradova, T.M., A.E. Lyashkov, W. Zhu, A.M. Ruknudin, S. Sirenko, D. Yang, S. Deo, M. Barlow, S. Johnson, J.L. Caffrey, et al. 2006. High basal protein kinase A-dependent phosphorylation drives rhythmic internal Ca2+ store oscillations and spontaneous beating of cardiac pacemaker cells. *Circ. Res.* 98:505–514. doi:10.1161/01.RES.0000204575.94040.d1

Zheng, J., M.D. Varnum, and W.N. Zagotta. 2003. Disruption of an intersubunit interaction underlies Ca2+-calmodulin modulation of cyclic nucleotide-gated channels. *J. Neurosci.* 23:8167–8175.